Problem of temperature dependence in the dynamic spin-fluctuation theory for strong ferromagnets

2008 J. Phys.: Condens. Matter 20 285205

(http://iopscience.iop.org/0953-8984/20/28/285205)

J. Phys.: Condens. Matter **20** (2008) 285205 (10pp) doi:10.1088/0953-8984/20/28/285205

Problem of temperature dependence in the dynamic spin-fluctuation theory for strong ferromagnets

B I Reser[1] **and N B Melnikov**[2,3]

[1] Institute of Metal Physics, Ural Branch of the Russian Academy of Sciences, 620041 Ekaterinburg, Russia
[2] Central Economics and Mathematics Institute of the Russian Academy of Sciences, 117418 Moscow, Russia
[3] Department of Computational Mathematics and Cybernetics, Moscow State University, 119992 Moscow, Russia

E-mail: reser@imp.uran.ru and melnikov@cs.msu.su

Received 4 September 2007, in final form 19 May 2008
Published 13 June 2008
Online at stacks.iop.org/JPhysCM/20/285205

Abstract
Temperature dependence of the magnetic characteristics of Fe and Fe–Ni Invar is considered in the dynamic nonlocal approximation of the spin-fluctuation theory. Calculations by several numerical methods show that the magnetic characteristics can have a discontinuous jump at high temperatures, well below the Curie temperature. Using the methods of catastrophe theory, we investigate the effect of small changes in the initial data on the results of the calculation. It is demonstrated that the discontinuous jump can only be smoothed but cannot be eliminated entirely without a significant change in the system of equations of the spin-fluctuation theory. Possible variants of such changes are discussed.

1. Introduction

Magnetic properties of transition metals and alloys at finite temperatures are usually calculated in the framework of various approximations of the spin-fluctuation theory (SFT) (see, e.g., [1–3] and references therein). A number of such approximations were developed in [4, 5] and fairly successfully applied first to ferromagnetic metals Fe, Co and Ni [6–8] and then to the Invar alloy Fe–Ni [9, 10].

The approximations [4, 5] are based on the functional integral method developed in [11, 12]. For the calculation of magnetic properties of strong ferromagnetic metals this method was first used in the static local approximation (SLA) in [13, 14]. Since even in the SLA the functional integral method is fairly complex, a number of significant simplifications were introduced in [13, 14]. In particular, the initial density of states (DOS) was always chosen in a simplified model form and the Fermi distribution was replaced by a step function[4]. The approximation [4] is also an SLA, but it uses the real band structure and advanced numerical methods for calculation of integrals involving the Fermi function [15] or its derivative [6]. However, in full accord with other SLA calculations the approximation [4] gives the magnetization that is not in sufficient agreement with the experiment, especially at low temperatures, gives a small effective moment in the Curie–Weiss law, etc. In this connection, in [5] the approximation [4] was extended to the case of dynamic nonlocal fluctuations.

The methods [4, 5] use a self-consistent quadratic approximation to the free energy of electrons in a random exchange field with averaging of the derivatives according to [16]. The zero-point fluctuations are taken into account in the initial DOS calculated by the density-functional method, and in the effective interaction constant U, determined from the experimental magnetic moment at $T = 0$. The thermal fluctuations are calculated self-consistently through the spin susceptibilities. Thus, the system of nonlinear equations solved in approximations [4, 5] of the SFT is considerably more complex than the standard one in the mean-field theory (see, e.g., [2, 17, 18]).

Calculations [4–10] showed that the solution to the system of equations of the SFT can be unstable at high temperatures,

[4] Moreover, in [14] the two-field model of spin fluctuations was used, which means neglecting the vectorial nature of the magnetic moment.

well below the Curie temperature, T_C. It is especially pronounced in Fe and Fe–Ni Invar, where spin fluctuations increase sharply in this region. Most often the instability takes the form of a discontinuous change of magnetic characteristics with temperature (the first-order-like transition). However, the discontinuous jump is usually too far from T_C to be interpreted in the framework of the critical phenomena. (See the theory for the critical region in, for example, [19, 20].)

The first-order phase transition in magnetization, m, in the critical region was observed in various versions [2, 21–23] of the self-consistent renormalization (SCR) spin-fluctuation theory developed for weak ferromagnetic metals. In the SCR calculations the jump in m was usually explained by the approximations done there. In particular, in phenomenological theory [21] it was related to the non-account of critical fluctuations, while in [2] to the approximative character of the theory [21] itself, even after its improvement by going from a *scalar* field for the spin density to a *vector* field, which is more realistic. In the theory [22] the first-order transition at T_C appeared in a simplified model for the longitudinal susceptibility $\chi_\parallel$. When the $\chi_\parallel$ was treated properly, this discontinuity was eliminated. Finally, in [23, 24] the problem of the fictitious first-order phase transition at T_C has been solved by taking into account the zero-point spin fluctuations in the SCR theory.

In *strong* ferromagnets, such as Fe and Fe–Ni Invar, the origin of the instability is unclear. Firstly, the approximations [4, 5] and those [2, 21–23] for *weak* ferromagnets employ different SFTs: the functional integral theory and SCR theory, respectively. Secondly, and above all, [4, 5] and [2, 21–23] consider the instability in different temperature ranges: over a wide range below T_C and in the narrow range near T_C, respectively. As is known [25], in the phase transition region the long-wave fluctuations play the predominant role. The nonlocal approximation [5] takes this fact into account, but insufficiently. Therefore, here we do not discuss the temperature dependence near T_C.

In the present paper, we study the discontinuous jumps in the temperature dependences of the magnetic characteristics in the dynamic nonlocal approximation (DNA) of the SFT by the example of Fe and Invar alloy $Fe_{0.65}Ni_{0.35}$. The outline of this paper is as follows. First, we demonstrate that the instability is not an artefact of the calculation method. To this end, we show that the coordinate bisection method used in [4–10] gives a good agreement with the multidimensional minimization over a wide range of temperatures. Second, through the calculation with the forward and backward changes of temperature, we demonstrate the hysteresis behaviour of the magnetic characteristics. This fact allows us to attribute the discontinuity in the temperature dependence to the system of equations of the SFT using the methods of catastrophe theory [26]. Next, we examine the effect of small changes of the initial data on the temperature dependences. This way we smooth the discontinuous change in the temperature dependence. Possible refinements of the approximations [4, 5] of the SFT are discussed in the conclusion.

Note that the problem of temperature dependence appears in the DNA of the SFT when the spin fluctuations increase sharply near T_C. In that case, the solution to the system of equations of the SFT becomes nonunique over a certain range of temperatures, i.e. the problem becomes ill-posed. Of the three solutions emerging in that range of the parameter T the middle one is unstable with any iterative procedure. In the Stoner and Heisenberg mean-field theories, with the single variable, magnetization[5], one does not encounter the problem: the magnetization curves are always smooth. In the presence of two or three variables (magnetization and spin fluctuations) the problem becomes much more complicated, and in a certain domain of the parameter T singularities may appear. They appear when the strong fluctuations and large magnetization are both present. Strong feedback of these quantities through the amplification factor (6) yields the instability.

In a sense, the degeneracy of the solutions near a phase transition is a general property of fluctuation theories (not only spin-fluctuation ones) [26]. However, the character of degeneracy depends strongly on the details of the specific theory; in particular, it depends on the way the anharmonicity and nonlocality of the fluctuations are taken into account.

Finally, the choice of the disordered Invar alloy $Fe_{0.65}Ni_{0.35}$ is not accidental. First, this alloy has a large content of Fe, and thus exhibits all the problems connected to a sharp increase of the fluctuations at high temperatures. Second, and most important, $Fe_{0.65}Ni_{0.35}$ is the alloy that, in our opinion, can explain the Invar problem *per se* (for a review see [27–30]).

2. Nonlinear system

The problem of calculation of the magnetic properties of transition metals at finite temperatures in the SFT is reduced to the solution of the system of four nonlinear integro-differential equations for the chemical potential μ, mean on-site spin moment s^z and mean square of the spin fluctuations ζ^x and ζ^z [5]:

$$\varphi_1(\mu, s^z, \zeta^x, \zeta^z) \equiv n_\uparrow + n_\downarrow - n_e = 0 \tag{1}$$

$$\varphi_2(\mu, s^z, \zeta^x, \zeta^z) \equiv (n_\uparrow - n_\downarrow)/2 - s^z = 0 \tag{2}$$

$$\varphi_3(\mu, s^z, \zeta^x, \zeta^z) \equiv UT/(2N\lambda_L^x)I^x - \zeta^x = 0 \tag{3}$$

$$\varphi_4(\mu, s^z, \zeta^x, \zeta^z) \equiv UT/(2N\lambda_L^z)I^z - \zeta^z = 0. \tag{4}$$

Here

$$n_\sigma = \frac{1}{\pi}\int \mathrm{Im}\, g_\sigma(\varepsilon) f(\varepsilon)\, \mathrm{d}\varepsilon \tag{5}$$

is the number of electrons with spin projection $\sigma = \uparrow, \downarrow$ or ± 1, n_e is the total number of electrons in the d band, U is the constant of the electron–electron interaction, T is the temperature (in energy units), N is the number of d bands (per atom and spin),

$$\lambda_L^\alpha = 1 - U\chi_L^\alpha(0) \qquad \alpha = x, z \tag{6}$$

and the function I^α, depending on the approximation of the SFT, i.e. static local (SL), static nonlocal (SN), dynamic

[5] The change of chemical potential is not critical.

local (DL) or dynamic nonlocal (DN), is calculated from the formulae

$$I^{\alpha}_{\mathrm{SL}} = 1 \tag{7}$$

$$I^{\alpha}_{\mathrm{SN}} = \frac{3}{b^3}\left(b - a\arctan\frac{b}{a}\right) \tag{8}$$

$$I^{\alpha}_{\mathrm{DL}} = \frac{2}{\pi}\arctan c_{\alpha} \tag{9}$$

$$I^{\alpha}_{\mathrm{DN}} = \int_0^1 \frac{1}{a_{\alpha}^2 + b_{\alpha}^2 k^2}\frac{2}{\pi}\arctan\frac{c_{\alpha}}{a_{\alpha}^2 + b_{\alpha}^2 k^2} 3k^2\,\mathrm{d}k. \tag{10}$$

In formulae (5)–(10) $\chi^{\alpha}_{\mathrm{L}}(0)$ is the local susceptibility (at zero frequency); $f(\varepsilon) = [\exp((\varepsilon-\mu)/T)+1]^{-1}$ is the Fermi function;

$$g_{\sigma}(\varepsilon) = \int \frac{\nu(\varepsilon')}{\varepsilon - \sigma\langle V_z\rangle - \Delta\Sigma_{\sigma}(\varepsilon) - \varepsilon'}\,\mathrm{d}\varepsilon' \tag{11}$$

is the mean single-site Green function, where $\nu(\varepsilon)$ is the nonmagnetic DOS, $\langle V_z\rangle = -Us^z$ is the mean exchange field and $\Delta\Sigma_{\sigma}(\varepsilon)$ is the fluctuation contribution to the self-energy part, calculated from the formula [4]

$$\Delta\Sigma_{\sigma}(\varepsilon) = \frac{g_{\sigma}(\varepsilon)\zeta^z}{1 + 2\sigma\langle V_z\rangle g_{\sigma}(\varepsilon)} + 2g_{\bar{\sigma}}(\varepsilon)\zeta^x \qquad \bar{\sigma}\equiv -\sigma; \tag{12}$$

$$a_{\alpha}^2 = \lambda_0^{\alpha}/\lambda_{\mathrm{L}}^{\alpha} \qquad \lambda_0^{\alpha} = 1 - U\chi_0^{\alpha}(0) \qquad b_{\alpha}^2 = (1 - a_{\alpha}^2)/0.6$$

$$c_{\alpha} = U\varphi_{\mathrm{L}}^{\alpha}\pi^2 T/(6\lambda_{\mathrm{L}}^{\alpha})$$

where $\chi_0^{\alpha}(0)$ is the static uniform susceptibility, and

$$\varphi_{\mathrm{L}}^{\alpha} = \left.\frac{\mathrm{d}\ \mathrm{Im}\,\chi_{\mathrm{L}}^{\alpha}(\varepsilon)}{\mathrm{d}\varepsilon}\right|_{\varepsilon=0}.$$

The quantities $\chi^{\alpha}_{\mathrm{L}}(0)$ and $\varphi^{\alpha}_{\mathrm{L}}$ are calculated from the formulae

$$\chi^x_{\mathrm{L}}(0) = -\frac{1}{\pi}\int \mathrm{Im}(g_{\uparrow}g_{\downarrow})\, f\,\mathrm{d}\varepsilon$$

$$\varphi^x_{\mathrm{L}} = \frac{1}{\pi}\int \mathrm{Im}\,g_{\uparrow}\ \mathrm{Im}\,g_{\downarrow}\left(-\frac{\partial f}{\partial\varepsilon}\right)\mathrm{d}\varepsilon$$

$$\chi^z_{\mathrm{L}}(0) = -\frac{1}{2\pi}\int (\mathrm{Im}\,g_{\uparrow}^2 + \mathrm{Im}\,g_{\downarrow}^2)\, f\,\mathrm{d}\varepsilon$$

$$\varphi^z_{\mathrm{L}} = \frac{1}{2\pi}\int [(\mathrm{Im}\,g_{\uparrow})^2 + (\mathrm{Im}\,g_{\downarrow})^2]\left(-\frac{\partial f}{\partial\varepsilon}\right)\mathrm{d}\varepsilon.$$

At $T < T_{\mathrm{C}}$ the quantities λ_0^x and λ_0^z are set to be zero. At $T > T_{\mathrm{C}}$ they are equal to each other, and the static uniform susceptibility $\chi_0^z(0)$ is defined using numerical differentiation of the spin moment s^z with respect to the magnetic field h (the mean field $\langle V_z\rangle$ is kept fixed):

$$\chi_0^z(0) = -\frac{\partial s^z}{\partial h} \simeq -\frac{s^z(\langle V_z\rangle + \Delta h/2) - s^z(\langle V_z\rangle - \Delta h/2)}{\Delta h}.$$

3. Solution methods

Consider a system of nonlinear equations in the n-dimensional Euclidean space:

$$\begin{aligned}\varphi_1(x_1, x_2, \ldots, x_n) = 0, \qquad & \varphi_2(x_1, x_2, \ldots, x_n) = 0,\\ \cdots \qquad & \varphi_n(x_1, x_2, \ldots, x_n) = 0.\end{aligned} \tag{13}$$

Let the system (13) have at least one solution such that its ith component belongs to the interval $[a_i, b_i]$, $i = 1, \ldots, n$.

3.1. Coordinate bisection method

First suggested in [31], the coordinate bisection method applies as follows[6]. Fix all the variables but the first one: $x_2 = a_2, \ldots, x_n = a_n$. Then $\varphi_1(x_1, a_2, \ldots, a_n)$ is a function of one variable x_1. In the interval $[a_1, b_1]$ by the bisection method find the root of the first equation of system (13), $x_1^{(1)}(a_2, a_3, \ldots, a_n)$. Compute the value of the function $\varphi_2(x_1^{(1)}, a_2, \ldots, a_n)$ at the left endpoint of the interval for x_2. Set $x_2 = b_2$ and find the root of the first equation of the system, $x_1^{(2)}(b_2, a_3, \ldots, a_n)$. Compute the value of the function φ_2 at the right endpoint of the interval for x_2 with the obtained 'new' x_1: $\varphi_2(x_1^{(2)}, b_2, a_3, \ldots, a_n)$. Continue with the bisection of the second equation and find the root $x_2^{(1)}(a_3, a_4, \ldots, a_n)$; in particular, the root x_1 is equal to a certain $x_1^{(k_1)}(x_2^{(1)}, a_3, \ldots, a_n)$. Compute the value of the third function $\varphi_3(x_1^{(k_1)}, x_2^{(1)}, a_3, a_4, \ldots, a_n)$ at the left endpoint for x_3. At $x_3 = b_3$ by the bisection method find the root of the second equation $x_2^{(2)}(b_3, a_4, \ldots, a_n)$; in particular, the root of the first equation is recalculated for the respective x_2 and x_3. Once x_1 and x_2 with fixed $x_3 = b_3$ are found, compute the value of the function $\varphi_3(x_1^{(k_1+k_2)}, x_2^{(2)}, b_3, a_4, \ldots, a_n)$ at the right endpoint for x_3. Continue the bisection method for the third equation and find the root $x_3^{(1)}(a_4, \ldots, a_n)$; in particular, $x_2^{(l_1)}(x_3^{(1)}, a_4, \ldots, a_n)$ and $x_1^{(k_1+k_2+\ldots+k_{l_1})}(x_2^{(l_1)}, x_3^{(1)}, a_4, \ldots, a_n)$ are calculated. Continue analogous calculations for the equations $\varphi_4, \ldots, \varphi_n$ and find $x_4, \ldots, x_n$. Thus, the solution of the system of nonlinear equations (13) reduces to a multiple solution of one-dimensional problems by the bisection method.

An advantage of the coordinate bisection method is that it does not use derivatives nor their approximations as opposed to quasi-Newton methods (see the next subsection). A large number of steps in the coordinate bisection method is not a serious weakness for the solution of the system (1)–(4) since the dimension of the system is not high and the computation time for the functions φ_i is small. We also remark that, to secure convergence of the method, it is necessary to specify the search domain with precision (for the details see [36]). Indeed, with the intervals $[a_i, b_i]$ too large, the solution cannot be found (in contrast to the one-dimensional bisection, where a root is always found once there is a sign change of the function). The specific character of the problem considered in the present paper allows us to choose the initial approximation at zero temperature with great precision, and the small step

[6] In the literature on numerical methods, we have not come across any generalizations of the bisection method to systems of equations.

size over the temperature ensures the proximity of the initial approximation in the successive calculations.

Since at fixed temperatures the spin fluctuations ζ^x and ζ^z are of the same order, a modification of the system of the SFT based on the transformation to the mean fluctuation (for the description see the appendix) has been successfully used in the coordinate bisection calculations [4–10].

3.2. Multidimensional minimization

As is well known, the solution of the system of nonlinear equations (13) can be reduced to minimization of the function

$$F(x_1, x_2, \ldots, x_n) = \sum_{i=1}^{n} (c_i \varphi_i(x_1, x_2, \ldots, x_n))^2 \qquad (14)$$

where c_i are the scale factor coefficients chosen according to the specific character of the problem. The function (14) is nonnegative and vanishes if and only if all the equations $\varphi_i(x_1, x_2, \ldots, x_n) = 0$ are valid.

To solve this problem one can use an iterative method. In the case of the simple iteration, from the explicit form of the functions φ_2, φ_3 and φ_4 in (2)–(4) we see that their values are exactly equal to the differences of the respective variables from the current and preceding steps:

$$\varphi_2(\mu_k, s_k^z, \zeta_k^x, \zeta_k^z) = s_k^z - s_{k-1}^z \qquad (15)$$

$$\varphi_3(\mu_k, s_k^z, \zeta_k^x, \zeta_k^z) = \zeta_k^x - \zeta_{k-1}^x \qquad (16)$$

$$\varphi_4(\mu_k, s_k^z, \zeta_k^x, \zeta_k^z) = \zeta_k^z - \zeta_{k-1}^z. \qquad (17)$$

We do not use the simple iteration method because of its low convergence rate. However, it is natural to assume that for another iterative minimization algorithm the relations (15)–(17) are satisfied approximately for the iterations close enough to the minimum point:

$$\varphi_2 \approx \Delta s^z \qquad \varphi_3 \approx \Delta \zeta^x \qquad \varphi_4 \approx \Delta \zeta^z. \qquad (18)$$

Hence the scale factor coefficients c_2, c_3 and c_4 are chosen in such a way that the magnitudes of $c_2\varphi_2$, $c_3\varphi_3$ and $c_4\varphi_4$ are approximately equal to the relative errors:

$$c_1 = 1 \qquad c_2 = 1/s^z(0)$$

$$c_3 = c_4 = 1/\langle V_z(0)\rangle^2 = 1/(U s^z(0))^2.$$

The value of c_1 is experience-based.

3.2.1. Quasi-Newton methods. The classical Newton's method for a function minimization operates as follows (see, e.g., [32, 33] for details). At the kth step, to refine the approximation $x^{(k)}$ of the local minimum x^* of the multivariable function $F(x)$ one constructs its quadratic Taylor approximation in the matrix-vector form:

$$F(x) \approx F(x^{(k)}) + (x - x^{(k)})^t \nabla F(x^{(k)}) + \tfrac{1}{2}(x - x^{(k)})^t \nabla^2 F(x^{(k)})(x - x^{(k)}) \qquad (19)$$

where x is the column vector $(x_1, \ldots, x_n)^t$, $\nabla F(x)$ is the gradient of the function F at the point x, i.e. the vector, whose ith component is equal to $(\nabla F)_i = \partial F/\partial x_i$, and $\nabla^2 F(x)$ is the Hessian matrix of the second partial derivatives of the function F at point x:

$$(\nabla^2 F)_{ij} = \frac{\partial^2 F}{\partial x_i \partial x_j}.$$

The minimum of the function (19) is attained at the point

$$x^{(k+1)} = x^{(k)} - [\nabla^2 F(x^{(k)})]^{-1} \nabla F(x^{(k)})$$

which is taken as the next initial approximation. Hence,

$$F(x^{(k+1)}) \approx F(x^{(k)}) - \tfrac{1}{2}(x^{(k+1)} - x^{(k)})^t \nabla^2 F(x^{(k)})(x^{(k+1)} - x^{(k)}).$$

Clearly the value of the function at the kth step decreases if the matrix $\nabla^2 F(x^{(k)})$ is positively defined. It is easy to show that Newton's method converges in a small enough neighbourhood of the local minimum if the function has continuous first and second derivatives. Moreover, the rate of convergence is quadratic.

Usually Newton's method is included in a more general procedure. This is motivated by the fact that far from the minimum point the matrix $\nabla^2 F(x^{(k)})$ cannot be positively defined, and thus the shift by the vector $-[\nabla^2 F(x^{(k)})]^{-1} \nabla F(x^{(k)})$ can, as well, not bring a decrease of the function. In that case the matrix $\nabla^2 F(x^{(k)})$ is replaced by a close symmetric positively defined matrix $B^{(k)}$. Positive definiteness of the matrix $B^{(k)}$ guarantees the decrease of the function: $F(x^{(k+1)}) < F(x^{(k)})$. The vector $\nabla F(x^{(k)})$ is also usually replaced by a finite-difference approximation. The methods of the second order that use approximations of the gradient of the function and approximations of the matrix of second derivatives instead of the precise values are called quasi-Newton methods.

3.2.2. Coordinate descent method. Multidimensional minimization of the function $F(x_1, x_2, \ldots, x_n)$ can be performed by a more slow but more reliable coordinate descent method. The gist of the method is as follows. As an initial approximation choose a point M_0 with coordinates $(x_1^{(0)}, x_2^{(0)}, \ldots, x_n^{(0)})$. Fix all the coordinates but the first one. Then $F(x_1, x_2^{(0)}, \ldots, x_n^{(0)})$ is a function of one variable, x_1. Solving the one-dimensional optimization problem for this function, we replace the point M_0 by the point $M_1 = (x_1^{(1)}, x_2^{(0)}, \ldots, x_n^{(0)})$, where the function F takes on the minimal value with respect to x_1, with other coordinates fixed. Now fix all the coordinates except for x_2, and consider F as the function of this coordinate, $F(x_1^{(1)}, x_2, x_3^{(0)}, \ldots, x_n^{(0)})$. Again, solving the one-dimensional optimization problem, we find its minimum point $x_2 = x_2^{(1)}$, that is $M_2 = (x_1^{(1)}, x_2^{(1)}, x_3^{(0)}, \ldots, x_n^{(0)})$. Similarly, the descent over the coordinates $x_3, x_4, \ldots, x_n$ is performed, then a new cycle from x_1 to x_n is started and so on. Finally, there is a sequence of the points $M_0, M_1, \ldots$ such that the values of the function F at these points form a nondecreasing sequence $F(M_0) \geqslant F(M_1) \geqslant \ldots$. The process stops when either the accuracy of the function or the accuracy of the arguments or the maximum number of iterations (cycles) is reached.

For smooth functions, given a good initial approximation, coordinate descent converges to the minimum. Among the

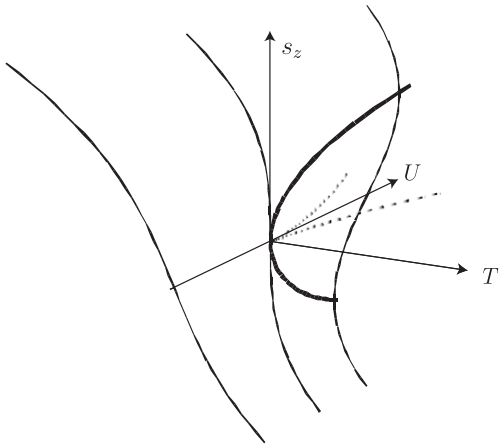

Figure 1. Sketch of the instability through the multiple solution. The projection (dotted line) of the set of all multiple solutions (heavy line) separates the domains with three solutions and one solution on the parameter plane.

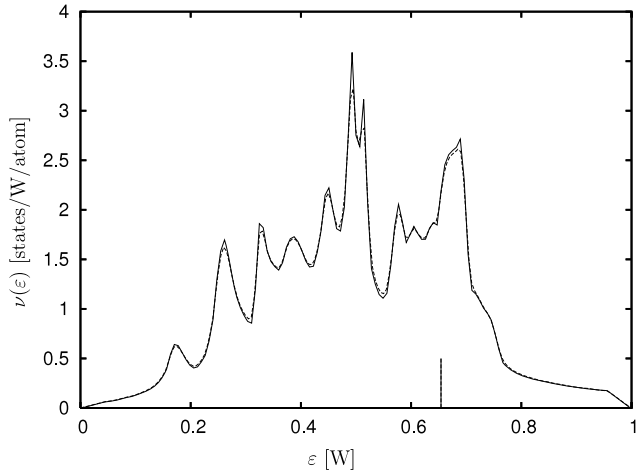

Figure 2. The DOS of the d band of non-magnetic $Fe_{0.65}Ni_{0.35}$, obtained from [37] (——), and the one smoothed out by convolution with the Lorentz function of the half-width $\Gamma = 0.001$ (− − −). The energy ε and half-width Γ are in units of the bandwidth $W = 9.70$ eV. The vertical line indicates the position of the Fermi level ε_F.

advantages of the coordinate descent is the possibility to use simple algorithms of one-dimensional optimization.

For one-dimensional optimization, we use the method that combines the golden section procedure with successive parabolic interpolation [34, 35]. The method is characterized by the quadratic rate of convergence in a neighbourhood of the minimum of a smooth function and a guaranteed linear rate of convergence in the case of a nonsmooth function with a nontrivial relief.

4. Instability through multiple solutions

In [36] we proved that the coordinate bisection method converges in a neighbourhood of a nondegenerate solution to a system of nonlinear equations. Therefore, the most probable cause of the instability in the system of equations (1)–(4) at high temperatures is the degeneracy, i.e. the determinant of the Jacobi matrix vanishes:

$$\det \left\| \frac{\partial(\varphi_1, \varphi_2, \varphi_3, \varphi_4)}{\partial(\mu, s^z, \zeta^x, \zeta^z)} \right\| = 0. \tag{20}$$

An explicit check of condition (20) is difficult since finite-difference approximations of the gradients lead to considerable loss of precision. An alternative approach is to demonstrate that locally the solution to the system of equations (1)–(4) becomes nonunique when the effective interaction constant U varies over an interval of its admissible values.

Consider the effective interaction constant U as an additional parameter to the temperature T. The existence of three solutions to the system of equations (1)–(4) is verified through the hysteresis behaviour of the solution components μ, s_z, ζ^x and ζ^z. With U fixed, the hysteresis in, say, s_z visualizes a jump down as T passes through a certain T_2, and a jump up as T passes through a T_1, $T_1 < T_2$, in the backward direction. Hence the curves $s_z(T)$, obtained through the forward and backward changes of temperature over $T_1 < T < T_2$, form a closed contour.

Mathematically, that means there are three solutions at the interval $T_1 < T < T_2$: two stable and one unstable in between them. At $T = T_1$ and $T = T_2$, a pair of adjacent solutions merges into a multiple one, which results in the degeneracy (20) of the system of equations (1)–(4). For $T < T_1$ and $T > T_2$, the system has only one solution, which is stable (for the details see [36]). Furthermore, if the interval (T_1, T_2), that encloses the hysteresis loop, collapses to a point T^* as U tends to a particular U^*, then the temperature dependence of each variable has an inflection point, where all the three solutions merge (in figure 1; for simplicity, the origin is translated to the inflection point (s_z^*, T^*, U^*)). To eliminate the instability near the inflection point a regularized version of the coordinate bisection method must be developed.

The above analysis yields that a small change of U can smooth out a discontinuous jump, which is half of a hysteresis loop, but a change over of the curvature in the temperature dependence may still persist.

5. Results and discussion

The numerical methods for solving a system of nonlinear equations are investigated in the DNA of the SFT, first, by the example of the Invar alloy $Fe_{0.65}Ni_{0.35}$. The initial non-magnetic DOS $\nu(\varepsilon)$ (figure 2) is formed from the two spin-polarized DOSs obtained from the self-consistent calculation for the disordered $Fe_{0.65}Ni_{0.35}$ [37]. A detailed description of $\nu(\varepsilon)$ formation is given in [10]. The experimental value of the spin magnetic moment per atom $m_0^{\exp} = 2Ns^z(0)\ \mu_B = 1.75\ \mu_B$ (where μ_B is the Bohr magneton), used to determine the effective interaction constant U, is taken from [38][7].

[7] Note that the experimental value $m_0^{\exp}$ cited in [38] is equal to 1.77 μ_B, but it includes a small (<0.1 μ_B) positive contribution of the orbital magnetic moment [39].

Table 1. The results of the calculation of the basic magnetic characteristics of the Invar $Fe_{0.65}Ni_{0.35}$ obtained by the coordinate bisection method and by the multidimensional minimization.

Temperature		Coordinate bisection				Multidimensional minimization				
T_W	T/T_C^{exp}	m_r	ζ_r^x	ζ_r^z	m_r^L	m_r	ζ_r^x	ζ_r^z	m_r^L	ITER
0.0000	0.000	1.000	0.000	0.000	1.000	1.000	0.000	0.000	1.000	1
0.0010	0.216	0.985	0.011	0.005	0.998	0.985	0.011	0.005	0.999	6
0.0020	0.433	0.942	0.040	0.019	0.994	0.943	0.040	0.019	0.994	12
0.0021	0.454	0.936	0.044	0.022	0.993	0.937	0.044	0.021	0.994	7
0.0022	0.476	0.928	0.049	0.024	0.992	0.930	0.048	0.024	0.993	8
0.0023	0.498	0.920	0.054	0.026	0.991	0.922	0.054	0.026	0.992	10
0.0024	0.520	0.912	0.060	0.029	0.990	0.913	0.059	0.029	0.991	13
0.0025	0.541	0.901	0.066	0.033	0.988	0.903	0.065	0.032	0.989	16
0.0026	0.563	0.889	0.073	0.036	0.987	0.891	0.072	0.036	0.988	21
0.0027	0.584	0.875	0.082	0.041	0.985	0.878	0.081	0.040	0.986	30
0.0028	0.606	0.860	0.091	0.046	0.983	0.862	0.090	0.045	0.984	45
0.0029	0.628	0.839	0.104	0.052	0.981	0.843	0.102	0.051	0.982	74
0.0030	0.649	0.813	0.118	0.060	0.978	0.819	0.115	0.059	0.980	137
0.0031	0.671	0.776	0.139	0.071	0.975	0.784	0.135	0.069	0.977	280

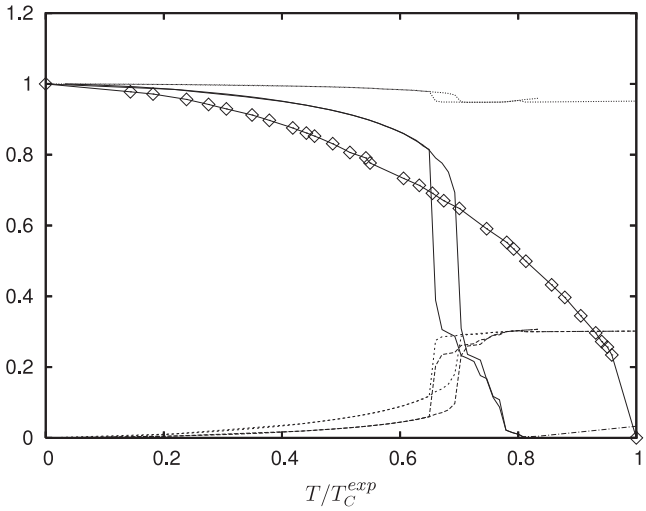

Figure 3. The magnetization $m(T)/m(0)$ (—— calculation, ◇◇◇◇ experiment [38]), the mean square of spin fluctuations ζ^x (- - - -) and ζ^z (– – –) in units of the square of the mean exchange field at $T = 0$, the reciprocal paramagnetic susceptibility $\chi^{-1}(T)$ (— · —) in units of T_C^{exp}/μ_B^2 and the local magnetic moment $m_L(T)/m(0)$ (· · · · · ·) of the Invar $Fe_{0.65}Ni_{0.35}$ calculated in the DNA of the SFT with $m_0^{exp} = 1.75\ \mu_B$ under forward and backward changes of temperature.

The results of the calculations of the basic magnetic characteristics of the Invar $Fe_{0.65}Ni_{0.35}$ obtained by the coordinate bisection method and via multidimensional minimization by the coordinate descent method are represented in figure 3 and in table 1. Since the most important physical parameter in the Invar problem is not the magnetization $m(T) = 2\ \mu_B s^z(T)$, but the local magnetic moment $m_L(T)$, calculated in the DNA by the formula [5]

$$m_L(T)/m(0) = [((Us^z(T))^2 + 2\zeta^x + \zeta^z)/(Us^z(0))^2]^{1/2}$$

it is also shown in the figure and table.

The investigation was carried out with the temperature T_W ranging from 0 to 0.01. (T_W is the temperature in units of the bandwidth $W = 9.70\,\text{eV} \approx 1.1 \times 10^5$ K.) First the temperature step is selected to be relatively large ($\Delta T_W = 0.001$), but as the values of the variables s^z, ζ^z and ζ^x start changing considerably, the programme switches to a smaller step size ($\Delta T_W/20 = 0.000\,05$).

Let us first analyse the results obtained by the coordinate bisection method. Calculation accuracies in the variables μ, s^z, ζ^x and ζ^z for one-dimensional bisections are selected to be

$$\delta_1 = 10^{-4} \qquad \delta_2 = 10^{-4} \times s^z(0) \approx 2 \times 10^{-5}$$
$$\delta_3 = \delta_4 = 10^{-4} \times (Us^z(0))^2 \approx 10^{-6} \tag{21}$$

so as to get relative errors of approximately the same order: 10^{-4} (see the explanation to the formula (18)).

As can be seen from figure 3 and table 1, at $T \leqslant 0.68\ T_C^{exp}$ a gradual increase of fluctuations and a smooth decrease of the magnetic moment are observed: during one small step in temperature the reduced fluctuations $\zeta_r^x = \zeta^x/\langle V_z(0)\rangle^2$ and $\zeta_r^z = \zeta^z/\langle V_z(0)\rangle^2$ increase by 0.001–0.01 and the reduced magnetic moment $m_r = s^z/s^z(0)$ decreases by 0.002–0.02[8]. The picture changes at temperatures $T \geqslant 0.69\ T_C^{exp}$. First an abrupt change in fluctuations and a jump down in the magnetic moment are observed, then the change in this quantities fails to be smooth. However, the preset accuracy of the solution to the system of equations (1)–(4) is retained at all temperatures.

It was the problem of instability of the solution to the system of equations (a jump down in the magnetic moment and abrupt change in fluctuations) that urged us to use the multidimensional minimization. The calculation was performed with the same initial data and at the same temperatures as in the one by the first method.

To minimize by the quasi-Newton method, we used the Fortran (double precision) routine UNCMND [35], which seeks a minimum of the function with line search. Results of the calculations did not give satisfactory agreement with the ones of the coordinate bisection method even in the temperature interval $T \leqslant 0.68\ T_C^{exp}$. Instead of the solution to $F(x) = 0$ the routine converges to a local minimum far off the

[8] In table 1, to be brief, we represent only every second set of values with the small step.

absolute one. It is necessary to note that the routine UNCMND does not give a user full control over the low level parameters (such as maximal step size). The routine also assumes that the function values are obtained accurately (to an accuracy comparable to the precision of the computer arithmetic). Since we aimed at implementing a reliable method that would work over a wide range of temperatures, we rejected the idea of tuning the quasi-Newton method. Instead, we implemented the coordinate descent method, which is slower but easier to control.

In the coordinate descent method the accuracy of the function (14) was chosen to be 10^{-7}. This value guarantees the relative errors over s^z, ζ^x and ζ^z to be nearly the same as in the calculation by the coordinate bisection method, i.e. within 10^{-3}–10^{-4}. As table 1 shows, at temperatures $T \leqslant 0.68\,T_{\mathrm{C}}^{\mathrm{exp}}$, the results obtained by the coordinate descent are in close agreement with the ones obtained by coordinate bisection (to the prescribed precision of 3–4 significant digits). However, starting from $T = 0.69\,T_{\mathrm{C}}^{\mathrm{exp}}$, the desired accuracy of the minimized function, 10^{-7}, cannot be reached even with the maximum number of cycles equal to 600, although a monotonic decrease of the magnetic moment and a monotonic increase of the fluctuations still persist.

It is important to note that the values of s^z, ζ^x and ζ^z obtained by coordinate descent practically coincide with the ones obtained by coordinate bisection over a wide temperature range (see table 1). This is a strong indication that the instability at high temperatures is related to the system itself rather than the solution method.

To demonstrate that the numerical instability at $T \geqslant 0.69T_{\mathrm{C}}^{\mathrm{exp}}$ is caused by the degeneracy of the system (1)–(4) near the left endpoint of this interval, we investigated a possibility of the hysteresis behaviour of the solution. The calculation with the forward and backward changes of temperature showed that, contrary to the experiment, the curves s^z, ζ^x and ζ^z have a small hysteresis loop (figure 3).

However, with the admissible initial magnetic moment $m_0^{\mathrm{exp}} = 1.70\ \mu_{\mathrm{B}}$ (see footnote 7), the constant of the effective interaction U is equal to 0.566 W (instead of $U = 0.582$ W for $m_0^{\mathrm{exp}} = 1.75\ \mu_{\mathrm{B}}$) and the hysteresis loop disappears (figure 4). The curves s^z, ζ^x and ζ^z obtained in the calculation with the backward change of temperature almost replicate the ones obtained with the forward calculation, except for small deviations in the instability region, and moreover these deviations do not have strictly vertical sections.

The simplest way to reduce the fluctuations ζ^α due to an implicit accounting for the higher terms of the expansion of the free energy $F(V)$ (formula (6) in [9]) consists in decreasing the effective interaction constant U in the quadratic term of the free energy, i.e. in the replacement of the constant U in formulae for the fluctuations ζ^α by $U_2 = cU$, where c is a parameter (slightly less than 1) estimated from experience. With $c = 0.985$ it is possible to obtain full agreement with experiment for the Curie temperature: $T_{\mathrm{C}} = 1.01T_{\mathrm{C}}^{\mathrm{exp}}$, for the paramagnetic Curie point: $\Theta_{\mathrm{C}} = 1.06T_{\mathrm{C}}^{\mathrm{exp}}$ and for the effective magnetic moment: $m_{\mathrm{eff}} = 0.97m_{\mathrm{eff}}^{\mathrm{exp}}$. But on the whole the curve for the magnetization does not fit the experimental one well enough. Qualitatively the calculated curve $m(T)$ stays similar to the one

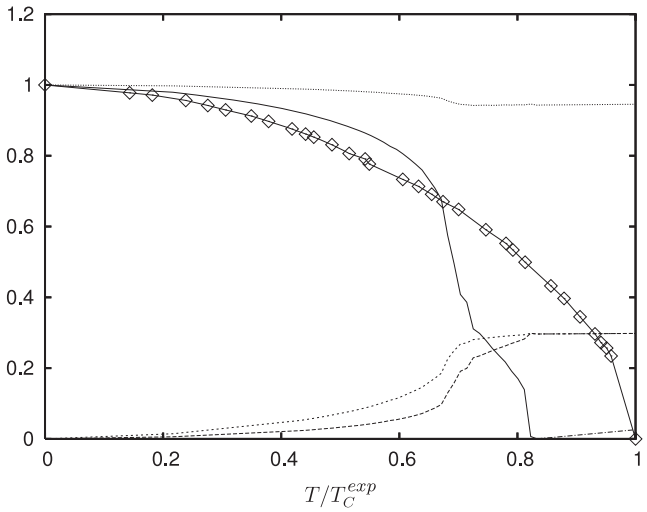

Figure 4. As figure 3, but calculated with $m_0^{\mathrm{exp}} = 1.70\ \mu_{\mathrm{B}}$.

obtained with $c = 1$ (figure 4), i.e. it still has the snake-like form. The reason is that the above change of the constant U yields a uniform change of the fluctuations, while to remove the 'snake' one has to account for the interaction between the fluctuations that becomes more intense with temperature[9].

In the SCR calculations [22], the first-order transition at T_{C} was eliminated entirely when the $\chi_\parallel^{-1}$ was approximated by $\chi_\perp^{-1}$ (the case $\eta = 0$ in (3.18) in [22]). However, in our calculation with $\zeta^z = \zeta^x$, the magnetic characteristics behaviour represented in figure 4 is retained. In [23, 24], to avoid the fictitious first-order transition in the SCR theory, a single equation for the longitudinal $\chi_\parallel$ and transverse $\chi_\perp$ susceptibilities was suggested. The relation that couples $\chi_\parallel$ and $\chi_\perp$ is based on the assumption that the total local spin fluctuation, i.e. the sum of the zero-point and thermal spin fluctuations, is conserved as it is in the Heisenberg local moment theory, and may be somehow justified for weak ferromagnets. In our case, the two equations for the fluctuations ζ^x and ζ^z are coupled to each other, as well as to the other two equations of system (1)–(4). However, system (1)–(4) is obtained using the quadratic approximation of the free energy, which does not account for the higher-order interaction (the anharmonicity of the fluctuations). Apparently, the coupling of the ζ^x and ζ^z in system (1)–(4) is insufficient.

Note that the temperature hysteresis is observed not only in the Fe–Ni Invar, but also in the usual Fe, i.e. it is a general problem for strong ferromagnets with sharply increasing spin fluctuations. To demonstrate that, we take as the initial DOS the one of non-magnetic Fe, calculated in the local-density approximation by the KKR method with a self-consistent potential [40]. Then the DOS is slightly smoothed out by convolution with the Lorentz function of half-width $\Gamma = 0.001W$ ($W = 7.16$ eV is the bandwidth) and normalized to one d band of unit width. With the help of smoothing we take into account the damping of one-electron states resulting

[9] The reduction of the fluctuations with the help of U_2 is formally equivalent to the change of the $\lambda(q, \omega)$ in the expression for the dynamical susceptibility (4.19) in [2] by a constant.

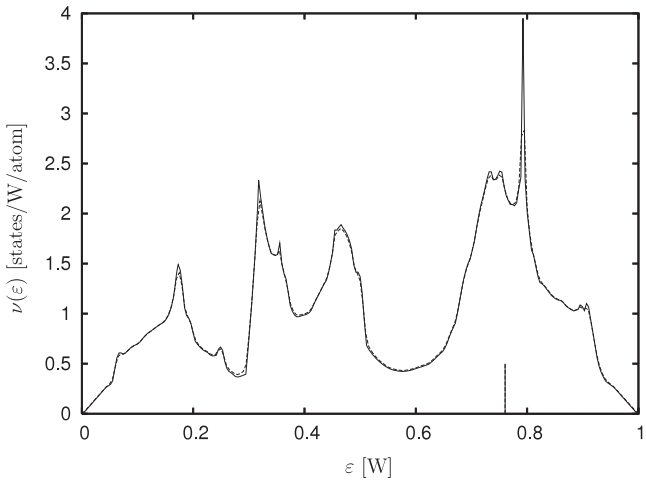

Figure 5. The DOS of the d band of non-magnetic Fe, calculated by the KKR method with a self-consistent potential (——), and the one smoothed out by convolution with the Lorentz function of half-width $\Gamma = 0.001$ (– – –). The energy ε and half-width Γ are in units of the bandwidth $W = 7.16$ eV. The vertical line indicates the position of the Fermi level ε_{F}.

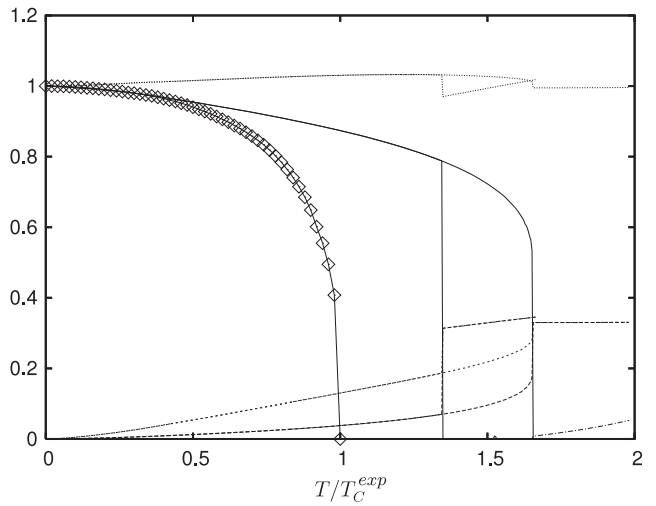

Figure 6. The magnetization $m(T)/m(0)$ (—— calculation, ◇◇◇◇ experiment [41]), the mean square of spin fluctuations ζ^x (- - - -) and ζ^z (— — —) in units of the square of the mean exchange field at $T = 0$, the reciprocal paramagnetic susceptibility $\chi^{-1}(T)$ (— · —) in units of $T_{\mathrm{C}}^{\mathrm{exp}}/\mu_{\mathrm{B}}^2$ and the local magnetic moment $m_{\mathrm{L}}(T)/m(0)$ (· · · · · ·) of Fe calculated in the DNA of the SFT with $m_0^{\mathrm{exp}} = 2.217\ \mu_{\mathrm{B}}$ under forward and backward changes of temperature.

from electron–electron correlations. The smoothed DOS of the d band $\nu(\varepsilon)$ used for calculation is represented in figure 5. The number of d electrons per atom $N_{\mathrm{e}} = Nn_{\mathrm{e}}$ is equal to 7.43. The effective interaction constant U determined from $m_0^{\mathrm{exp}} = 2.217\ \mu_{\mathrm{B}}$ [41] is $0.741W$. As can be seen from figure 6, which shows the results of our calculation for the magnetic characteristics in the forward and backward changes of temperature, in Fe the hysteresis loop is even larger than in the Fe–Ni Invar.

However, the temperature behaviour of magnetization near the jump in the Fe–Ni Invar and Fe is qualitatively different (compare figures 3 and 6). In the former, the magnetization does not jump down to zero, i.e. the switching-over to the paramagnetic state does not occur. Therefore, in Fe–Ni Invar, a small change of the initial data only smears the discontinuous jump into a smooth curve with an inflection (see section 4). In contrast, in the case of Fe, the smoothing could transform the first-order transition to the second-order one.

Finally, as an alternative attempt to eliminate the discontinuous jump, we carried out calculations for Fe and Fe–Ni Invar with the longitudinal or transverse fluctuations only. As should be expected, the switching-off of the transverse or longitudinal fluctuations yields a Curie temperature almost twice as large as the experimental one. Worse agreement with experiment is achieved, in this case, for other magnetic characteristics as well. Most importantly, the use of models with a one-dimensional fluctuating field does not solve the problem of temperature dependence for Fe and Fe–Ni Invar. In particular, in the model accounting for longitudinal fluctuations only, the magnetization decreases too slowly with the increase in temperature and the discontinuous jump (first-order transition) turns out to be too sharp. In the model accounting for transverse fluctuations only, the magnetization decreases faster and agreement with experiment at low temperatures is achieved, but singularities of the magnetization curve remain.

6. Conclusions

Calculations of the magnetic properties of Fe and Fe–Ni Invar in the DNA of the SFT showed that the coordinate bisection method is quite applicable to practical calculations at finite temperatures. The instability at high temperatures is connected not with the solution method—the two different numerical methods gave well-agreed results—but with the system of nonlinear equations itself.

The problem is that in Fe and in alloys with a considerable content of Fe, like Fe–Ni Invar, the spin fluctuations at high temperatures increase sharply, which means the parameters $\lambda_{\mathrm{L}}^{\alpha} = 1 - U\chi_{\mathrm{L}}^{\alpha}(0)$ tend to zero. Consequently, there is a strong dependence of the solution to the system of nonlinear equations (1)–(4) on the accuracy of the effective constant U and the static local susceptibility $\chi_{\mathrm{L}}^{\alpha}(0)$[10].

Note that the problem of temperature dependence is connected not only with the system of equations, but also with the initial parameters dependent on the real ferromagnet (the DOS $\nu(\varepsilon)$, the number of d electrons n_{e}, the effective interaction constant U, etc). Each particular set of data yields its own solution to the system of nonlinear integro-differential equations (1)–(4). For example, in Co and Ni no instabilities were found at all (see, e.g., [6]). Even in the case of Fe and Fe–Ni Invar, reasonable changes of the initial data and/or the system of equations can either remove or at least reduce considerably the effect of the instability. Finally, as our calculations show, with only longitudinal fluctuations taken into account the discontinuous jump near T_{C} only increases, i.e. accounting for both transverse and longitudinal fluctuations does not worsen the situation, as stated in [43], but improves it.

[10] High sensitivity of the local magnetic characteristics of iron to the value of U at high temperatures is well illustrated in [42].

Apparently, for transition metals and alloys with strong spin fluctuations and large magnetization, the approximation [5] of the SFT should be improved to be equally applicable at high temperatures. It is necessary to exceed the limits of the quadratic approximations for the free energy of electrons in the fluctuating exchange field $F(V)$ and for the fluctuation contribution to the self-energy part $\Delta\Sigma$. Quite possible, a more consistent account—not only in the derivation of the formula (10)—of the short-range magnetic order is necessary. Work in this direction is underway. We expect that the reduction of the sharp increase in the fluctuations by means of the terms of higher order in the expansions of $F(V)$ and $\Delta\Sigma$ and a consistent account of the short-range order will allow us not only to eliminate the instability of the solution but also, which is more important, will allow us to improve the agreement with the experiment at high temperatures.

As regards the original coordinate bisection method for solving the system of nonlinear equations and the method for the analysis of the instability domain, which are numerically justified in the present paper (and analytically in [36]), they can be of interest by themselves.

Acknowledgments

BIR is grateful to V I Grebennikov and V Ya Raevskii for useful discussions. We thank the referees of the paper for constructive criticism.

This work was supported in part by the Russian Science Support Foundation and the Russian Foundation for Basic Research (grant nos. 06-01-00148 and 08-01-00685).

Appendix. Modified system of equations of the SFT

Instead of the spin fluctuations ζ^x and ζ^z, we introduce the mean value $\bar{\zeta} = (2\zeta^x+\zeta^z)/3$ and the difference $\Delta\zeta = \zeta^x-\zeta^z$ (recall that $\zeta^y = \zeta^x$). Substituting

$$\zeta^x = \bar{\zeta} + \Delta\zeta/3 \qquad \zeta^z = \bar{\zeta} - 2\Delta\zeta/3 \tag{A.1}$$

we transform the initial system (1)–(4) into an equivalent one

$$\tilde{\varphi}_1(\mu, s^z, \bar{\zeta}, \Delta\zeta) = 0 \tag{A.2}$$

$$\tilde{\varphi}_2(\mu, s^z, \bar{\zeta}, \Delta\zeta) = 0 \tag{A.3}$$

$$\tilde{\varphi}_3(\mu, s^z, \bar{\zeta}, \Delta\zeta) \equiv (2\tilde{g}_3(\mu, s^z, \bar{\zeta}, \Delta\zeta) + \tilde{g}_4(\mu, s^z, \bar{\zeta}, \Delta\zeta))/3 - \bar{\zeta} = 0 \tag{A.4}$$

$$\tilde{\varphi}_4(\mu, s^z, \bar{\zeta}, \Delta\zeta) \equiv \tilde{g}_3(\mu, s^z, \bar{\zeta}, \Delta\zeta) - \tilde{g}_4(\mu, s^z, \bar{\zeta}, \Delta\zeta) - \Delta\zeta = 0 \tag{A.5}$$

where $g_3(\mu, s^z, \zeta^x, \zeta^z) = UT/(2N\lambda_{\mathrm{L}}^x)I^x$ and $g_4(\mu, s^z, \zeta^x, \zeta^z) = UT/(2N\lambda_{\mathrm{L}}^z)I^z$, and the tilde stands for the result of the substitution (A.1). Now, instead of system (A.2)–(A.5), we solve the system of the first three equations (A.2)–(A.4), as if $\Delta\zeta$ were fixed, while at each step $\Delta\zeta$ is refined by simple iterations of the last equation from the formula

$$\Delta\zeta_{k+1} = \tilde{g}_3(\mu_k, s_k^z, \bar{\zeta}_k, \Delta\zeta_k) - \tilde{g}_4(\mu_k, s_k^z, \bar{\zeta}_k, \Delta\zeta_k)$$

where $k = 0, 1, 2, \ldots$ is the number of the step of the solution algorithm for the system (A.2)–(A.4), and $\bar{\zeta}_0$ and $\Delta\zeta_0$ are taken from the calculation with the preceding value of the temperature.

References

[1] Moriya T (ed) 1981 *Electron Correlation and Magnetism in Narrow-Band Systems* (Berlin: Springer)
[2] Moriya T 1985 *Spin Fluctuations in Itinerant Electron Magnetism* (Berlin: Springer)
[3] Capellmann H (ed) 1987 *Metallic Magnetism* (Berlin: Springer)
[4] Rezer B I and Grebennikov V I 1997 *Phys. Met. Metallogr.* **83** 127
[5] Rezer B I and Grebennikov V I 1998 *Phys. Met. Metallogr.* **85** 20
[6] Reser B I 1999 *J. Phys.: Condens. Matter* **11** 4871
[7] Reser B I 2000 *J. Phys.: Condens. Matter* **12** 9323
[8] Reser B I 2002 *J. Phys.: Condens. Matter* **14** 1285
Reser B I 2003 *J. Magn. Magn. Mater.* **258/259C** 51
[9] Reser B I 2004 *J. Phys.: Condens. Matter* **16** 361
[10] Rezer B I 2007 *Phys. Met. Metallogr.* **103** 357
[11] Stratonovich R L 1957 *Dokl. Akad. Nauk SSSR* **115** 1097
Stratonovich R L 1958 *Sov. Phys.—Dokl.* **2** 416 (Engl. Transl.)
[12] Hubbard J 1959 *Phys. Rev. Lett.* **3** 77
[13] Hubbard J 1979 *Phys. Rev.* B **19** 2626
Hubbard J 1979 *Phys. Rev.* B **20** 4584
[14] Hasegawa H 1979 *J. Phys. Soc. Japan* **46** 1504
Hasegawa H 1980 *J. Phys. Soc. Japan* **49** 178
[15] Reser B I 1996 *J. Phys.: Condens. Matter* **8** 3151
[16] Hertz J A and Klenin M A 1974 *Phys. Rev.* B **10** 1084
[17] Kim D J 1999 *New Perspectives in Magnetism of Metals* (New York: Kluwer–Academic)
[18] Kübler J 2000 *Theory of Itinerant Electron Magnetism* (Oxford: Clarendon)
[19] Hertz J A 1971 *Int. J. Magn.* **1** 253
[20] White R M 2007 *Quantum Theory of Magnetism* (Berlin: Springer)
[21] Murata K K and Doniach S 1972 *Phys. Rev. Lett.* **29** 285
[22] Lonzarich G G and Taillefer L 1985 *J. Phys. C: Solid State Phys.* **18** 4339
[23] Takahashi Y 1986 *J. Phys. Soc. Japan* **55** 3553
[24] Takahashi Y 2001 *J. Phys.: Condens. Matter* **13** 6323
[25] Landau L and Lifshitz E M 1985 *Statistical Physics, Course on Theoretical Physics* vol 5 (New York: Pergamon)
[26] Poston T and Stewart I 1998 *Catastrophe Theory and its Applications* (New York: Dover)
[27] Wassermann E F 1990 *Ferromagnetic Materials* vol 5, ed K H J Buschow and E P Wohlfarth (Amsterdam: Elsevier Science) p 237
[28] Wassermann E F 1991 *J. Magn. Magn. Mater.* **100** 346
[29] Shiga M 1994 *Materials Science and Technology* vol 3B, part II ed R W Cahn, P Haasen and E J Kramer (Weinheim: VCH) p 159
[30] Wittenauer J (ed) 1997 *The Invar Effect: A Centennial Symposium* (Warrendale, PA: The Minerals, Metals and Materials Society)
[31] Rezer B I 1994 *Phys. Met. Metallogr.* **77** 451
[32] Gill P E, Murray W and Wright M H 1981 *Practical Optimization* (London: Academic)
[33] Dennis J E Jr and Schnabel R B 1983 *Numerical Methods for Unconstrained Optimization and Nonlinear Equations* (Englewood Cliffs, NJ: Prentice-Hall)
[34] Forsythe G E, Malcolm M A and Moler C B 1977 *Computer Methods for Mathematical Computations* (Englewood Cliffs, NJ: Prentice-Hall)
[35] Kahaner D, Moler C and Nash S 1989 *Numerical Methods and Software* (Englewood Cliffs, NJ: Prentice-Hall)
[36] Melnikov N B and Reser B I 2008 *Proceedings of Dynamic Systems and Applications* vol 5 (Atlanta, GA: Dynamic Publishers)
[37] Johnson D D, Pinski F J and Stocks G M 1985 *J. Appl. Phys.* **57** 3018

[38] Crangle J and Hallam G C 1963 *Proc. R. Soc.* A **272** 119
[39] Scott G G 1962 *J. Phys. Soc. Japan* **17** (Suppl. B I) 372
Reck R A 1974 *Phys. Rev.* B **5** 2381
[40] Moruzzi V L, Janak J F and Williams A R 1978 *Calculated Electronic Properties of Metals* (New York: Pergamon)
[41] Crangle J and Goodman G M 1971 *Proc. R. Soc. Lond.* A **321** 477
[42] Prokopjev Yu I and Reser B I 1991 *J. Phys.: Condens. Matter* **3** 6055
[43] Takahashi Y 2006 *J. Phys.: Condens. Matter* **18** 521